Polyion Complex Langmuir−Blodgett Layers Containing an Ionic Water-Soluble Polysilane

Takahiro Seki,*,† Atsushi Tohnai,‡ Nobutaka Tanigaki,§ Kiyoshi Yase,§ Takashi Tamaki,§ and Akira Kaito§

Research Laboratory of Resources Utilization, Tokyo Institute of Technology, 4259 Nagatsuta, Midori-ku, Yokohama 226, Japan, Fine Chemicals Research Center, Catalysts and Chemical Industries Company Ltd., 1-13 Kitaminato-cho, Wakamatsu-ku, Kitakyushu 808, Japan, and National Institute of Materials and Chemical Research, 1-1 Higashi, Tsukuba, Ibaraki 305, Japan

Received April 12, 1996; Revised Manuscript Received December 19, 1996[⊗]

ABSTRACT: Monolayers of anionic amphiphiles, arachidic acid ($C_{19}COOH$) and a double long chain sulfonic acid derivative ($2C_{12}SO_3Na$), were spread on the water subphase containing an ammonium-containing polysilane (APS), and Langmuir−Blodgett (LB) films from these polyion complex monolayers were prepared. Single layer deposition of these polyion complex monolayers was successfully achieved onto a hydrophilic substrate under all conditions examined, but multilayers could be prepared under limited conditions in the Z-type mode. The UV absorption spectra of the transferred $C_{19}COO(H)$/APS monolayers indicated that the conformational state of APS in the films are dependent on the subphase pH. The absorbance of the transferred LB films confirmed that the APS is incorporated monomolecularly on the lifting process. Polarized UV absorption spectra revealed no preferential orientation of the APS backbone in the LB films. The multilayers formed in the Z-type deposition were eventually inverted to stacked bilayer structure (Y-type layers) after aging and successive annealing, as proven by the small angle X-ray reflectometry. LB films composed of $2C_{12}SO_3^-$/APS possessed a more refined layer structure with a more smooth surface than those of $C_{19}COO(H)$/APS, probably due to a better dimensional matching of the APS unit and the cross section of the amphiphile. Finally, structural features of the $C_{19}COO(H)$/APS polyion complex LB film were discussed in comparison with those of a homologous amphiphilic material reported previously (Seki et al. *Macromolecules* **1995**, *28*, 5609).

Introduction

Research on polyion complex formation of a charged amphiphile monolayer with a gegenionic polyelectrolyte at the air−water interface started probably from the work of Goddard and Hannan in 1976.[1] About 10 years later, the practical importance of the polyion complexation at the interface was pointed out by Shimomura and Kunitake.[2] They showed that Langmuir−Blodgett (LB) deposition becomes successful by polyion complexation for charged amphiphiles which encounter difficulties in the ordinary LB procedures.[2,3] Ever since, a number of works on this class of LB films have been undertaken from both viewpoints of technical applications[2−6] and structural characterizations.[7−16]

To date, a great deal of data have been accumulated on the packing state of the amphiphile as well as surface structures in the polyion complex LB films, which can be evaluated by Fourier transform infrared spectroscopy (FTIR),[7] X-ray photoelectron spectroscopy (XPS),[8,9] X-ray diffraction,[8−10] and so forth. With regard to characterizations of polyion complex monolayers at the air−water interface, UV−visible absorption analysis of the amphiphile,[11] fluorescence microscopy,[12,13] scanning probe microscopy,[14] surface plasmon spectroscopy,[15] and neutron reflectometry[16] have been carried out.

Despite the above efforts, little knowledge has been obtained on the polyelectrolyte component in the LB films regarding the conformation and orientation. Such information would be available if the polyelectrolyte component is selectively probed in a spectroscopic method. Use of a polysilane material seems promising for this purpose since the Si-catenated backbone, although being flexible like ordinary polyelectrolyte, exhibits strong light absorption in the UV region due to the σ-electron conjugation. The transition moment of the $\sigma-\sigma^*$ absorption band is parallel to the chain direction, and the band gap is sensitive to the populational ratio of the *trans*/*gauche* conformers.[17] These optical properties are anticipated to shed light on the main chain orientation and conformational states. We have recently developed a series of ammonium-containing polysilanes.[18−20] The materials having a long alkylammonium moiety, like other chemically functionalized polysilanes,[21−23] are amphiphilic and found to be successfully assembled as multilayers by the ordinary LB technique.[18−20] On the other hand, a compound with a trimethylammonium group (APS, Chart 1) becomes water-soluble,[24,25] and this material would be used as the polyelectrolyte component in the polyion complex LB films.

This paper describes our detailed study on the preparation and structural characterization of mono- and multilayered polyion complex LB films containing APS.[24] The anionic amphiphiles used in this study are icosanoic acid (arachidic acid, $C_{19}COOH$) or sodium 1,2-bis-[(dodecyloxy)carbonyl]ethane-1-sulfonate ($2C_{12}SO_3Na$) (Chart 1). Structural characterizations of these ion-complexed monolayers and LB films were carried out by UV absorption spectroscopy, FTIR spectroscopy, X-ray reflectometry, and transmission electron microscopy (TEM). Closely related LB films composed of an amphiphilic analogue, $C_{18}APS$ (see Chart 1) have already been described[20] (designated as PS1 in the previous paper). The previous data with this amphiphilic polysilane are likely to give useful implications in the present study.

† Tokyo Institute of Technology. Phone and fax: +81-45-924-5247. E-mail: tseki@res.titech.ac.jp.
‡ Catalysts and Chemical Industries Co. Ltd.
§ National Institute of Materials and Chemical Research.
⊗ Abstract published in *Advance ACS Abstracts,* March 1, 1997.

S0024-9297(96)00548-7 CCC: $14.00

Chart 1

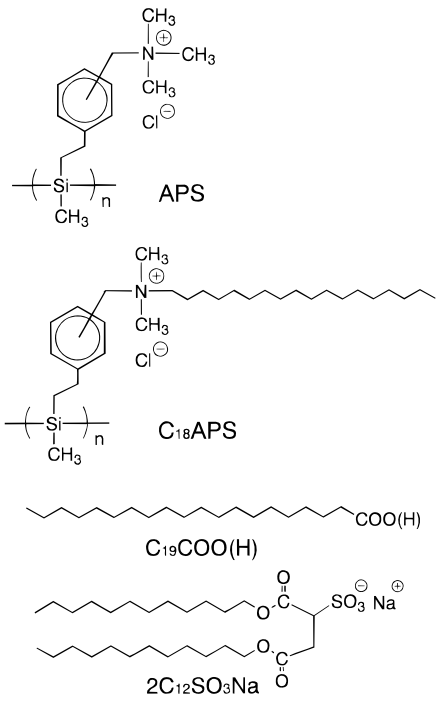

Experimental Section

Materials. Arachidic acid ($C_{19}COOH$) was purchased from Sigma Chemical Co. and used without further purification. Sodium 1,2-bis[(dodecyloxy)carbonyl]ethane-1-sulfonate ($2C_{12}$-SO_3Na) was obtained from Sogo Pharmaceutial Co. and recrystallized once from ethyl acetate before use. Chloroform as the spreading solvent was of Merck spectroscopic grade.

Preparation of APS[24,25] and C_{18}APS[20] was described previously. Both polysilanes were derived by quarternization of a common precursor material, a quantitatively chloromethylated poly[methyl(β-phenethyl)silane] ($M_w = 21\,000$, $M_w/M_n = 1.30$).[20]

Quartz plates were cleaned as described previouly.[26] For transmission IR spectrum measurements CaF_2 crystal plates ($10 \times 3 \times 1$ mm, OKEN) were used. These substrates were subjected to an ozone treatment using an ORC VUM-3073-B UV dry processor prior to use.

Methods. Observation of the spreading behavior of monolayers and their transfer onto quartz substrates were performed by a Lauda FW-1 film balance at 21 °C under dim red light. The anionic amphiphiles were spread from chloroform solution at a concentration of ca. 1×10^{-3} mol dm^{-3} onto an APS containing (1×10^{-5} unit mol dm^{-3}) water subphase. pH changes of the subphase for $C_{19}COO(H)$ monolayers were attained by adding appropriate amounts of 1 N hydrochloric acid or sodium hydroxide solutions. The sodium chloride (1.0×10^{-2} mol dm^{-3}) was commonly involved in the subphase in these experiments to minimize the influence of changes in the ionic strength upon pH adjustment. The subphase thus prepared contains approximately a 50-fold excess amount of the Si unit to the amphiphile molecules at the interface.

UV−visible absorption spectra were taken at room temperature using a JASCO HSSP3 spectrophotometer. For polarized UV−visible spectrum measurements, a Glan-Thomson type polarizer was placed in front of the specimen. FTIR measurements were carried out at room temperature with a Perkin-Elmer System 2000 at a resolution of 2 cm^{-1}.

X-ray diffraction profile in the reflection geometry was obtained with a Rigaku RU-300 at room temperature. The specimens were scanned at 0.2 °C/min using Cu Kα radiation monochromatized by pyrolyzed graphite.

The morphological observation by the transmission electron microscopy (TEM) was performed as follows. A monolayer at the air−water interface was deposited onto a glass substrate by the horizontal lifting (touching) method. The films on the substrate were covered and reinforced by vacuum-deposited carbon film with a thickness of ca. 3 nm. The films were stripped off from the substrate in distilled water or diluted hydrofluoric acid solution, and the floating films were transferred onto Cu grids. The film morphology was observed with a Zeiss CEM-902 at an accelerating voltage of 80 kV.

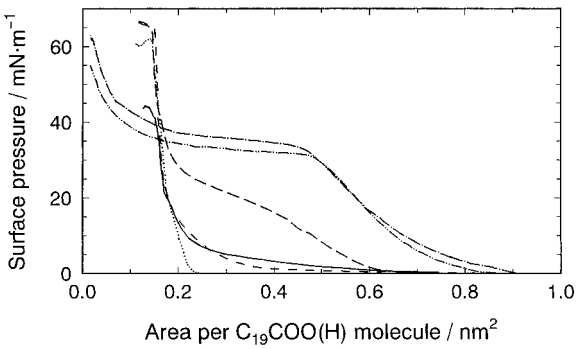

Figure 1. Surface pressure−area curves of $C_{19}COO(H)$ at 20 °C on an aqueous subphase containing APS (1×10^{-5} mol dm^{-3}) and NaCl (1×10^{-2} mol dm^{-3}). $C_{19}COOH$ was spread at pH 2.0 (—), 5.0 (- - -), 9.1 (— —), 10.2 (—·—), and 12.0 (—··—). The dotted curve (···) shows the compression curve of $C_{19}COO$-(H) at pH 7 in the absence of APS.

Results and Discussion

1. Polyion Complex Formation at the Air−Water Interface and Transfer onto Substrates. 1.1. Spreading Behavior. Figure 1 presents the spreading behavior of $C_{19}COO(H)$ monolayers on an APS-containing subphase at various pHs. Coincidence of the ionic strength should be of importance since this can influence the electrostatic interaction behavior between a charged polymer and a gegenionic insoluble monolayer, as suggested by neutron reflection detection[16] and a theoretical simulation.[27] The monolayers showed significant expansion from that of a pure $C_{19}COO(H)$ monolayer (dotted line), indicative of the ionic complexation between the $C_{19}COO(H)$ monolayer and APS at the air−water interface. The shape of the surface pressure−area (π-A) curves was strongly dependent on the subphase pH. In lower pH regimes below 5, the monolayer gave the lift-off area of ca. 0.6 nm^2 per $C_{19}COOH$ molecule and the limiting areas obtained by extrapolation of the steepest curve regions to zero pressure were ca. 0.2 nm^2. On the other hand, the monolayer further expanded in high pH regimes above 10. The lift-off area shifted to regions above 0.8 nm^2, and the compression curves showed a plateau at 30−40 mN m^{-1} below 0.5 nm^2. A collapse of the monolayer probably occurs in this plateau region. An intermediate behavior was observed for the monolayer at pH 9.1.

The above pH dependent character of the spreading behavior of the $C_{19}COOH$ monolayer should be the consequence of changes in the dissociation state of the carboxylic acid head group. It is reasonably explained that a more effective electrostatic interaction is attained at more dissociated states, and this causes the film expansion. The full deprotonation of the carboxylic acid is thus attained at a pH above 10. We previously reported on the results of these monolayer systems in the range of pH 2.0−8.0.[24] As shown here, deprotonation of carboxylic acid is therefore insufficient within the previous pH conditions. The π-A curves of the polyion complexed monolayers at pHs 10 and 12 are similar in shape to that of C_{18}APS on pure water which also gives a plateau near 40 mN m^{-1} with a somewhat smaller lift-off area (see Figure 1a in ref 20). Therefore,

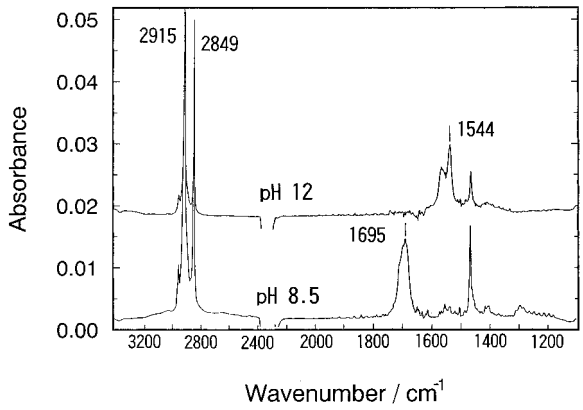

Figure 2. Transmission FTIR spectra of 25-layered $C_{19}COO$-(H)/APS LB films transferred onto a CaF_2 plate at 5 mN m^{-1} and pH 8.5 and 12.0.

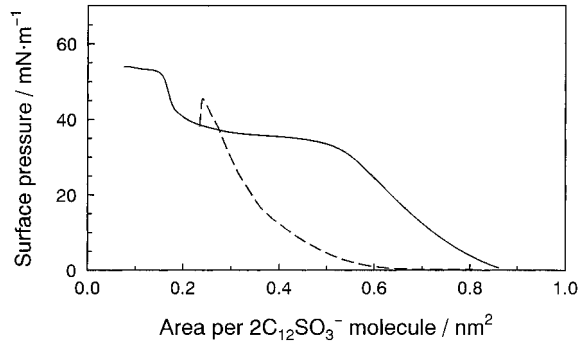

Figure 3. Surface pressure−area curves of $2C_{12}SO_3Na$ at 20 °C on pure water in the absence (broken line) and presence of APS (1×10^{-5} mol dm^{-3}, solid line).

the spreading characteristics of the fully ion complexed $C_{19}COO^-$/APS monolayer are almost equivalent to those of the C_{18}APS monolayer.

The dissociation states of the carboxylic acid head group in the polyion complex LB films were confirmed by transmission FTIR analysis. The IR spectra of 25-layered $C_{19}COO(H)$/APS LB films (for transfer conditions, see below) on a CaF_2 plate are displayed in Figure 2. The C═O stretching band for the film transferred at pH 8.5 showed dual bands peaked at 1695 and ca. 1540 cm^{-1}, which are assigned to the bands for carboxylic acid and carboxylate forms, respectively. The spectrum for the film transferred at pH 12, in contrast, indicated the fully dissociated form of carboxylate, giving a maximum at 1544 cm^{-1}, and no signal of free carboxylic acid was observed.

The π-A curves of the double-chained $2C_{12}SO_3Na$ monolayers are indicated in Figure 3. For these systems, the experiments were carried out only at neutral pH without sodium chloride. Similarly to $C_{19}COO(H)$ systems, the curve exhibited a significant expansion when APS was involved in the subphase. The limiting area of the $2C_{12}SO_3^-$ monolayer on pure water was ca. 0.4 nm^2, which is reasonably the doubled value of the single-chained $C_{19}COO(H)$. Upon addition of APS, the shape of the π-A curve exhibited a considerable expansion which closely resembled those of $C_{19}COO^-$/APS monolayers observed at pH 10 and 12. Thus, the number of the long alkyl chain in the amphiphile made little influence on the molecular occupying area. It is therefore assumed that the bulky Si unit of APS contributes dominantly to the observed area of the polyion complex monolayers.

1.2. Transfer onto Solid Substrates. Transfer of a single layer of polyion-complexed monolayers was successfully achieved (transfer ratio > 0.9) onto a clean hydrophilic substrate surface (quartz or CaF_2) in the vertical dipping method for both amphiphiles and under all pH conditions employed. However, repeated depositions for assembling multilayers were attainable only under limited conditions. For the series of $C_{19}COO(H)$/APS monolayers, multilayer deposition could be carried out at pH regions above pH 8. The surface pressure applied was low (5 mN m^{-1}) due to poor stability of these monolayers at higher pressures (e.g. 25 mN m^{-1}; see section 1.3). At low pressures the LB multilayers were deposited only in the process of upstroke lifting (Z-type mode deposition). On the other hand, the multilayer transfer of $2C_{12}SO_3^-$/APS was possible at surface pressures above 20 mN m^{-1}. In this case, again, the multilayers were formed in the Z-type deposition.

In both cases, the transfer ratio became less at greater repetition stages above five cycles. Refined layer structures, therefore, would not be anticipated from this transfer behavior. The polar structure of these multilayered LB films formed by the Z-type deposition should be thermodynamically unstable. As supposed, the structure of the LB multilayer changed by long-term storage at room temperature and more definitely by a thermal annealing treatment (see section 3.2).

1.3. Morphology of the Monolayer. The morphology of the polyion complex monolayer was observed by TEM. Figure 4 indicates TEM images of $C_{19}COO(H)$/APS monolayers deposited at neutral pH and the surface pressures of 5 (a and b) and 25 (c and d) mN m^{-1}. These images were taken in the normal (a and c) and electron spectroscopic (b and d) modes. In the electron spectroscopic mode, the beam was filtered at 285 eV. This allows images showing an abundance of carbon atoms: The brighter parts in the micrographs indicate regions where carbon atoms are more abundant. Normal TEM images (a and c) show that the monolayers were almost homogeneous, but the electron spectroscopic images (b and d) revealed the high heterogeneity of these films. At 5 mN m^{-1} where most of the LB deposition was achieved, the monolayer film was almost homogeneous but exhibited some domain structure having featureless contours of a few micrometers scale. The monolayer at 25 mN m^{-1} was found to be highly heterogeneous, exhibiting a number of wrinkles of several micrometer lengths which seem to start from circular domains. The direction of stripes of the wrinkles was orthogonal to the compression direction. As stated in section 1.2, the deposition of this monolayer was not successful at 25 mN m^{-1} due to poor stability. These TEM images support the fragile nature of the monolayer at high pressures. Lee et al.[13] observed a similar morphology by a fluorescence microscope for a double chain amphiphile monolayer complexed with a polyelectrolyte in a collapsed region.

2. UV Absorption Spectra and Conformational States of Transferred Monolayers. The UV−visible absorption spectra of $C_{19}COO(H)$/APS monolayers on both sides of a quartz substrate transferred at pH 2−12 were indicated in Figure 5. The $\sigma-\sigma^*$ absorption band of the Si backbone ranged from 285 to 293 nm and was a function of the subphase pH. Absorbance of the LB films changed concomitantly. Absorbance values obtained in the higher pH regimes (ca. 0.006) were in good agreement with that observed for C_{18}APS films.[20] This consistency confirms that APS is *monomolecularly*

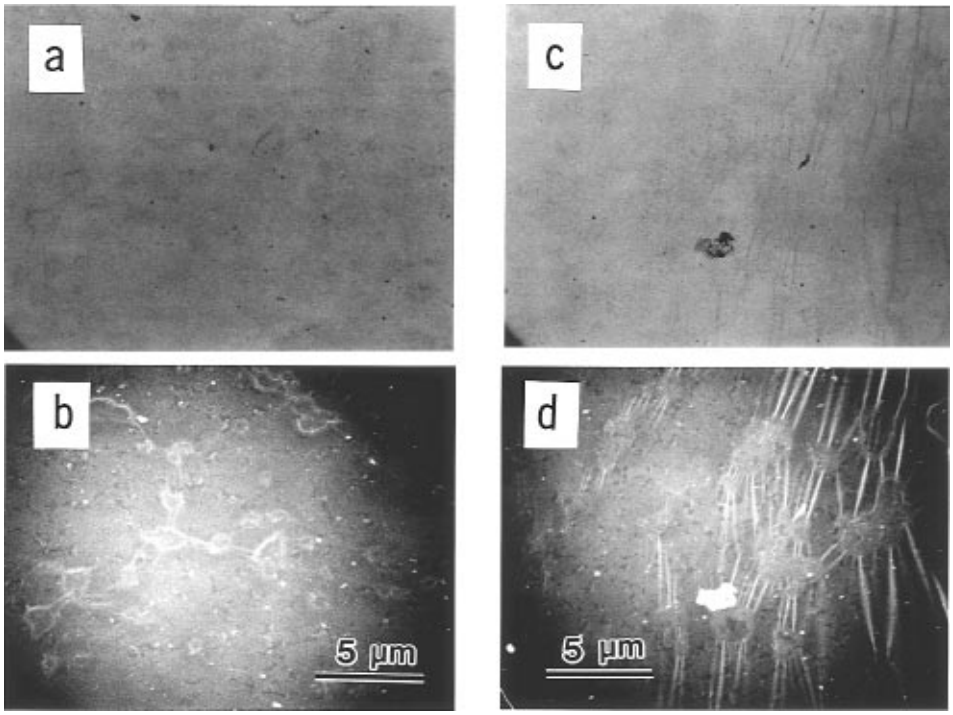

Figure 4. TEM images of $C_{19}COO(H)$/APS monolayers transferred at 5 (a and b) and 25 mN m^{-1} (c and d) by the horizontal lifting method. Micrographs were taken in normal (a and c) and electron spectroscopic (filtered at 285 eV) image (b and d) modes in the identical field.

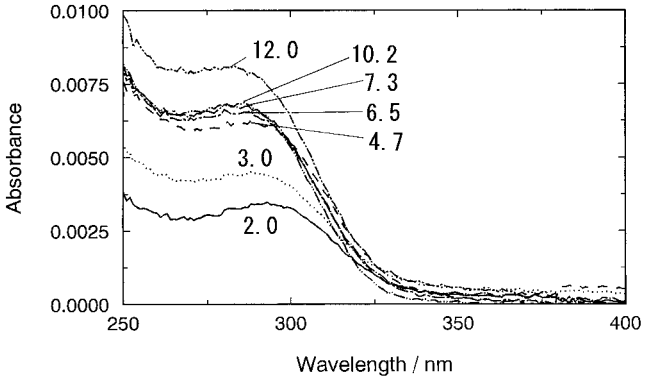

Figure 5. UV absorption spectra of single LB monolayers on both sides of a quartz plate transferred at 5 mN m^{-1} at various pHs. The pH of the subphase was 2.0 (—), 3.0 (···), 4.7 (— —), 6.5 (—·—), 7.3 (—·—), 10.2 (—··—), and 12.0 (—··—).

incorporated into the polyion complex LB films. Formerly, Takahara et al.[9] demonstrated the formation of stoichiometric complexation in polyion complex LB films by XPS analysis, and our UV spectroscopic data support this stoichiometric relation.

Figure 6 presents the peak position of the UV spectra (a) and absorbance at these wavelengths (b) as a function of pH. With increasing pH, the absorption band exhibited hypsochromic shifts. The band shifts should reflect changes in the conformational state of the Si backbone of APS.[18−20] Absorbance at the peak wavelength decreased in acidic regions, indicating that amounts of transferred APS are reduced.

Changes in the optical properties indicated above should be closely coupled with changes in the dissociation state of the carboxylic acid moiety of the $C_{19}COOH$ monolayer on the water surface. On the basis of the above spectroscopic observations,[18−20] the following model which is schematically drawn in Figure 7 can be assumed. The conformational state of electrostatically absorbed APS is influenced by the changes in the two-

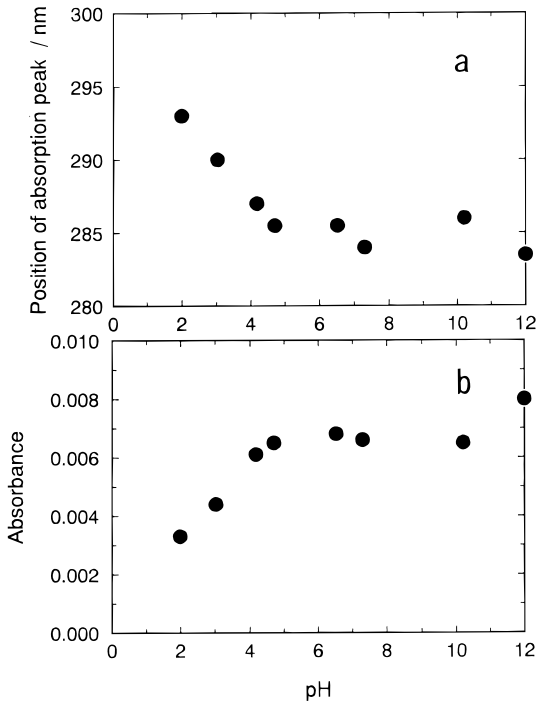

Figure 6. Maximum wavelengths of the $\sigma-\sigma^*$ band of APS in the polyion complex LB monolayers (a) and absorbance at these wavelengths (b) as a function of subphase pH.

dimensional density of anionic charge, namely the protonation state of the carboxyl head group, beneath the $C_{19}COO(H)$ monolayer. At low pHs, the backbone of APS is relatively extended, containing more *trans* conformers from a requirement of stoichiometric charge neutralization with diluted anionic charges of the $C_{19}COO(H)$ monolayer. At higher pHs, on the other hand, the anionic charge density increases, and the ion-complexed APS backbone is folded and crowded more. The amount of absorbed APS increases at higher pHs accordingly. For the $2C_{12}SO_3^-$/APS LB film, the ab-

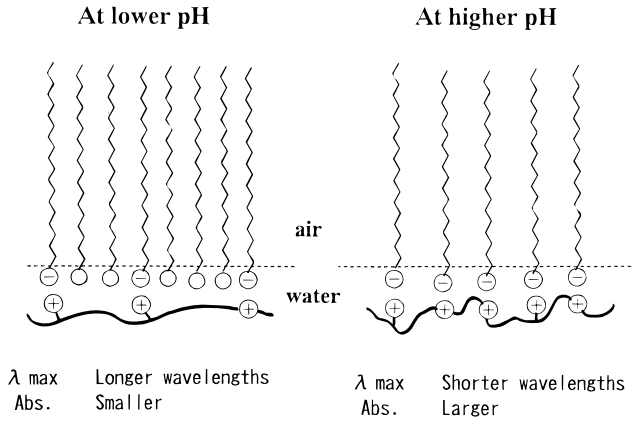

Figure 7. Oversimplified representation of the ion complexation state of APS with the $C_{19}COO(H)$ monolayer at the air−water interface for the explanation of the observed pH dependency in the optical properties.

sorption peak was positioned at a relatively longer wavelength (293 nm). This is probably due to the larger occupying area for the double chain amphiphile.

Both the absorption peak and absorbance profiles in Figure 6 showed an inflection at pH 4−5. This pH region nearly corresponds to the pK_a of *n*-alkanecarboxylic acid (4.8) at room temperature. Kobayashi et al.[28] conducted an XPS study to determine the amount of divalent metal ions incorporated into the LB films as a function of the subphase pH. According to their data, with increasing pH, the metal ions start to be involved exactly in this pH region. It can be thus assumed that the conformational state and the deposited amount of APS is primarily influenced by the dissociation near the intrinsic pK_a. However, the overall apparent dissociation constant of this monolayer is substantially shifted to a higher value. As stated in section 1.1, the full deprotonation of $C_{19}COOH$ monolayers required high basic conditions above pH 10. Interestingly, the optical properties of APS were influenced only in the acidic pH region below 5, but not in the neutral to basic pH regions where the majority of carboxylic acid groups are dissociated, as seen in the FTIR data (Figure 2).

The absorption peak of APS in pure water is positioned at 280−286 nm.[25,29] Therefore, the $\sigma-\sigma^*$ absorption band of $C_{19}COO(H)$/APS monolayers transferred at acidic pHs and the $2C_{12}SO_3^-$/APS monolayer are shifted to longer wavelengths. These results can be compared with those observed for the binding process of an anionic surfactant, sodium dodecyl sulfate (SDS), to APS in a water solution.[29] Binding of SDS to APS induces bathochromic spectral shifts in a similar fashion.

3. Structure of LB Multilayers. 3.1. On the Orientation of the APS Main Chain. The LB deposition procedure of the vertical dipping frequently induces an in-plane main chain orientation of polysilane materials in LB films.[18−23] Figure 8 depicts the polarized UV−visible absorption spectra of two-layered LB films of $C_{19}COO(H)$/APS deposited at pH 8.0 (a) and five-layered $2C_{12}SO_3^-$/APS (b). UV spectra taken in the parallel and perpendicular polarization with respect to dipping direction essentially agreed with each other for both films, indicating that no preferential orientation in the backbone was attained in these LB films. We have observed a preferred orientation for C_{18}APS LB films in the direction of the dipping direction.[18−20] This main chain orientation in the C_{18}APS films is probably

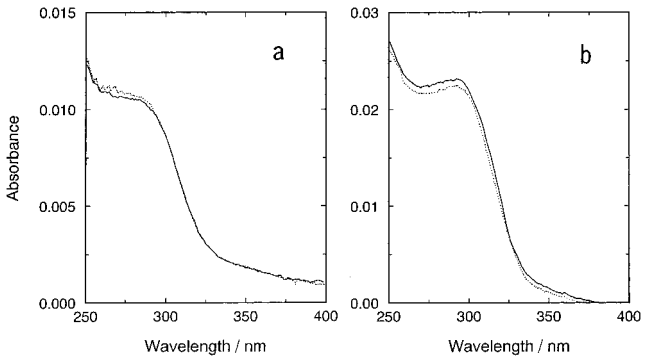

Figure 8. Polarized UV absorption spectra of 2-layered $C_{19}COO(H)$/APS (a) and 5-layered $2C_{12}SO_3^-$/APS (b) on both sides of a quartz plate with normal incidence. Polarization of the probing beam was set parallel (solid line) and perpendicular (dotted line) to the dipping direction.

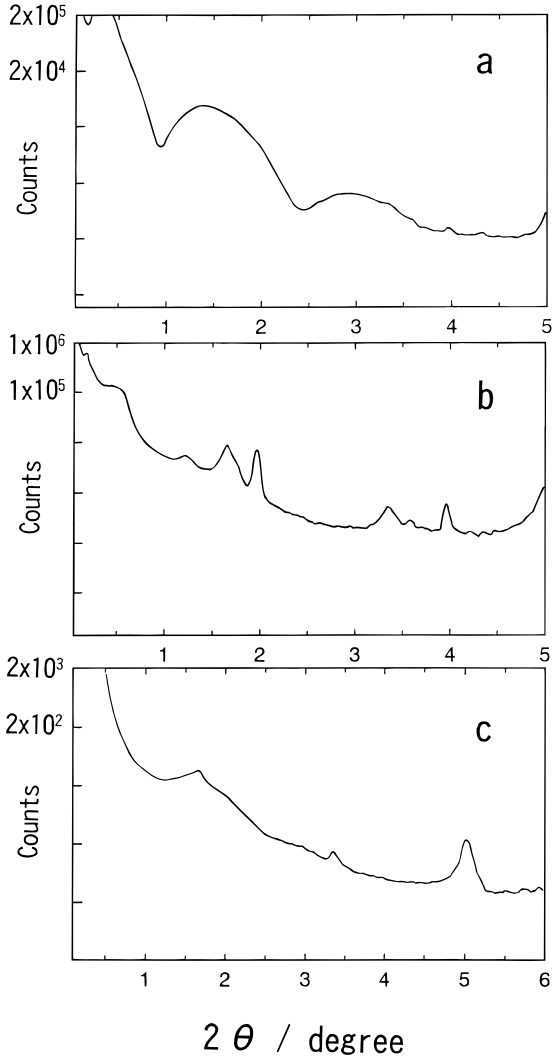

Figure 9. Small angle X-ray reflection profiles of a 20-layered $C_{19}COO(H)$/APS LB film deposited at 5 mN m^{-1} on a quartz plate. The measurements were achieved within 2 weeks after deposition (a), after 3 months (b), and after annealing at 80 °C for 12 h (c).

attained by a flow effect on the water surface.[30] We will discuss this point in the last part of section 3.3.

3.2. X-ray Diffractometry. X-ray diffraction patterns of typical examples are presented in Figures 9 and 10 for 20-layered $C_{19}COO(H)$/APS and $2C_{12}SO_3^-$/APS films, respectively. Layer spacings (*d*) and overall film thicknesses (*L*) evaluated from Bragg peaks and Kiessig

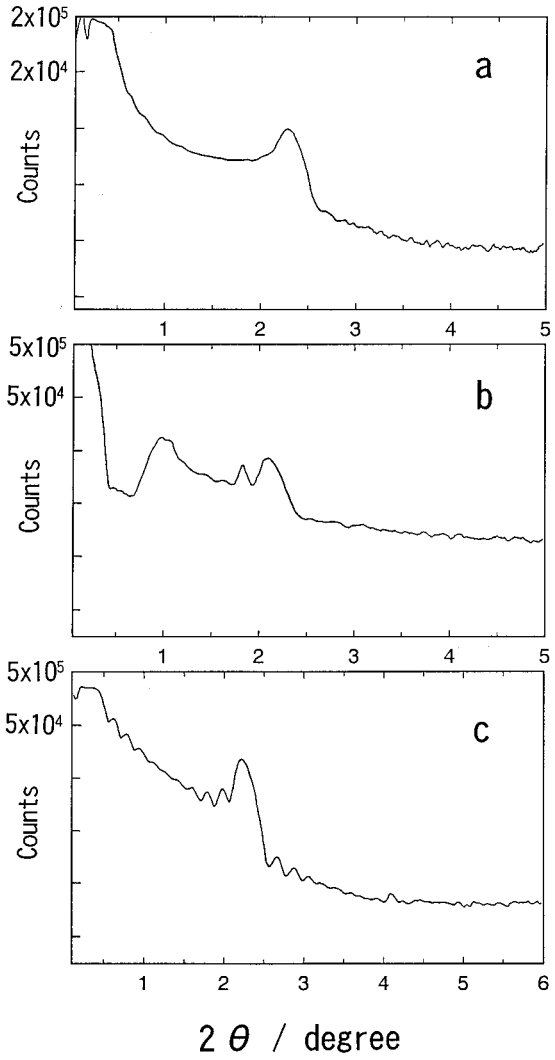

Figure 10. Small angle X-ray reflection patterns of 20-layered $2C_{12}SO_3^-$/APS LB films deposited at 25 mN m^{-1} on a quartz plate. The measurements were achieved within 2 weeks after deposition (a), after 3 months (b), and after annealing at 80 °C for 12 h (c).

Table 1. X-ray Diffraction Data

LB film	d^a/nm	L^b/nm
$C_{19}COO(H)$/AMP (pH 8, 20 layers)		
fresh[d]	(broad)	—[c]
aged[e]	4.48, 5.35, 7.30	—
annealed[f]	5.31	—
$C_{19}COO^-$/AMP (pH 12, 20 layers)		
fresh	(broad)	—
aged	(broad)	—
annealed	(broad)	—
$2C_{12}SO_3^-$/APS (10 layers)		
fresh	4.11	27.4
aged	4.12, 4.21	—
annealed	4.13	29.0
$2C_{12}SO_3^-$/APS (20 layers)		
fresh	3.85	—
aged	3.95, 4.15	—
annealed	4.03	46.3

[a] Layer spacing determined from Bragg peaks. [b] Overall film thickness determined from Kiessig fringes. [c] No Kiessig fringes were observed. [d] Measured within 2 weeks. [e] Kept at room temperature for 3 months. [f] Annealed at 80 °C for 12 h in an oven.

fringes, respectively, are summarized in Table 1. Three patterns in the figures show the results of experiments carried out within 2 weeks after LB deposition (a), after storing for 3 months at room temperature (b), and after annealing at 80 °C for 12 h (c). The layer structure of these polyion complex films clearly changed with aging and annealing processes. The multilayers were deposited in the Z mode, but typical values eventually obtained for the layer spacings, d were ca. 5.3 and 4 nm for $C_{19}COO(H)$/APS and $2C_{12}SO_3^-$/APS LB films, respectively, indicate the structure of stacked bilayers. An inversion process from the Z-type polar multilayers to thermally stable Y-type stacked bilayers should have occurred consequently.

Kiessig fringes were observed for a couple of samples of the $2C_{12}SO_3^-$/APS system, which reveals sufficient smoothness of the film surface. Overall thicknesses obtained did not coincide with the multiplication of the bilayer length with the supposed deposition number. This should result from the poor transfer ratios at repeated deposition cycles (see section 1.2).

The fresh sample of $C_{19}COO(H)$/APS LB film transferred at pH 8 (Figure 9a) gave very broad and distorted Bragg peaks with which the layer spacing could not be determined. When the film was aged, several diffraction peaks appeared (Figure 9b). Mainly three kinds of peaks corresponding to $d = 4.48$, 5.35, and 7.30 nm were observed. The final annealed film (Figure 9c) gave a single layer spacing ($d = 5.35$ nm). Therefore, among the three peaks for the aged film, the most thermally stable layer structure had the spacing of 5.35 nm. The $C_{19}COO(H)$/APS films deposited at pH 8 showed a first-order Bragg peak; however, that transferred at pH 12 is highly disordered and the determination of the layer spacing was impossible. A very close value of the layer spacing was reported for cadmium arachidic acid ($C_{19}COO{\cdot}^1/_2Cd^{2+}$) LB multilayers (5.4−5.5 nm).[31] Given that the long alkyl chains are in the *trans-zigzag* conformation (see section 3.3, arguments on IR data), the alkyl chains should be more tilted in the $C_{19}COO(H)$/APS LB films than in the $C_{19}COO{\cdot}^1/_2Cd^{2+}$ multilayer in consideration of the insertion of APS.

Multilayers of $2C_{12}SO_3^-$/APS were better structured, and the pattern changes after the aging and annealing were smaller. This is probably due to a better dimensional matching between the APS unit and the occupying area of the $2C_{12}SO_3^-$ monolayer. The fresh sample gave a diffraction pattern which shows a broadened but clear Bragg peak corresponding to 3.85 nm spacing which is overlapped with weak Kiessig fringes (Figure 10a). Similarly to the $C_{19}COO(H)$/APS film, the aging process led to a more complicated pattern giving an additional Bragg peak of 4.15 nm spacing (Figure 10b). After annealing, this film exhibited a refined layer structure giving a single layer spacing ($d = 4.03$ nm). For the annealed film, clear fringes were overlaid in the Bragg peaks. Kajiyama et al.[9] reported the structure of a relating polyion complex film composed of $2C_{14}SO_3^-$ (a homologue of $2C_{12}SO_3^-$ having two tetradecyl chains) and poly(ethyleneimine) (PEI) which was deposited above 30 mN m^{-1}. The small angle X-ray diffraction pattern of $2C_{14}SO_3^-$/PEI film indicated a layer spacing of 5.31 nm with a tilt angle of 5° from the surface normal. A comparison of the spacing could be made with the film containing $2C_{12}SO_3^-$ if the length of four methylene groups (ca. 0.56 nm) for the bilayer is subtracted. The final spacing of the observed $2C_{12}SO_3^-$/APS film (4.03 nm) is smaller than that expected from this calculation (4.75 nm). The length occupied by the amphiphile in each layer should be even smaller in consideration of the larger dimension of the APS unit compared to that of PEI unit. We assume a consider-

able tilt of the long alkyl chain part in the $2C_{12}SO_3^-$/APS film.

3.3. Structural Features of the Amphiphilic and Polyion Complex LB Films. We have already reported a relevant LB work using ammonium-containing amphiphilic polysilane homologues.[20] Among them, the features and properties of C_{18}APS having a single long chain can be properly compared with those of the present polyion complex LB films. The essential difference in the chemical structure between C_{18}APS and C_{19}COO(H)/APS is the linkage mode that connects the alkyl chain to the ammonium group, namely covalent and ionic bonds, respectively.

Notable features of the C_{18}APS in the monolayers and LB multilayers can be summarized as follows: (i) the monolayer on the water surface is sufficiently stable even at high-pressure regions for transfer (e.g., 30 mN m^{-1}), (ii) the transfer is performed in the Y mode, (iii) both the monolayers and LB multilayers are fully homogeneous, as proven by TEM observation even in the electron spectroscopic mode, (iv) the surfaces of the multilayers were more highly smooth, which is characterized by the appearance of clear Kiessig fringes, and (v) a preferential orientation of the Si main chain in the dipping direction is observed in the multilayers. Good stability and transfer behavior (i and ii) may result from the covalent bond between the long chain and the ammonium moiety in our systems. However, this is not fully understood since many of the polyion complex LB films have been prepared at relatively high surface pressures (above 20 mN m^{-1}), and a repeated transfer process does not lessen the transfer ratios. Instability of the C_{19}COO(H)/APS monolayer is probably due to unmatched proportions between the size of the APS unit and the cross section of C_{19}COOH. In fact, the film transfer was improved when the larger double chain amphiphile ($2C_{12}SO_3Na$) was employed. The features of C_{18}APS films concerning (iii) and (iv) should originate from the thoroughly amorphous nature. The morphological heterogeneity of the C_{19}COO(H)/APS film (Figure 4), in contrast, seems to stem from a partial crystallization of the C_{19}COOH monolayer.

In the FTIR spectra (Figure 2), the asymmetric and symmetric C−H stretching bands of the long alkyl chains of the C_{19}COO(H)/APS LB film were observed at 2915 and 2849 cm^{-1}, respectively, and were not changed by the pH conditions of deposition (pH 8.5 and 12). These low-frequency peaks reasonably indicate that the long alkyl chains are in the *trans-zigzag* conformation in both films.[32,33] In contrast, a 43-layered C_{18}APS LB multilayer gave C−H asymmetric and symmetric stretching peaks at higher frequencies of 2922 and 2853 cm^{-1}, respectively, indicative of disordered packing of the alkyl chains involving a considerable amount of *gauche* conformers.[20] For C_{18}APS LB films, we have proposed a structural model from FTIR and X-ray data in which the Si main chain is located within the hydrocarbon array of stacked bilayers. For the present polyion complex film, in contrast, this model would be inadequate judging from the packing state of the alkyl chains fixed in the *trans-zigzag* conformation. The Si backbone of APS in the polyion complex film is possibly positioned between the hydrophilic ends of the C_{19}COO(H) layers, as one may expect in polyion complex LB films.

Finally, the complete absence of the backbone orientation with respect to the dipping direction in the polyion complex LB films is worth mentioning. The orientation mechanism is generally understood by a deposition-induced flow of monolayer on the water surface.[30] Two explanations for the present result may be possible. First, the monolayers of C_{19}COO(H) and $2C_{12}SO_3^-$ complexed with APS form rigid solidlike states and possess little fluidity, and the monolayer flow on the water surface should not be reflected in the orientation of the absorbed polymer. Rigidity of the ion complex monolayer is implied from the FTIR data that the hydrocarbon chains are fixed in the *trans-zigzag* conformation. Second, if the ion exchanging between the anionic amphiphile and APS occurs at a fast or comparable rate, this can also diminish or cancel a flow-induced orientation.

Summary

This work was undertaken to extend the utility of polysilane derivatives to the research of polyion complex LB films, in particular, aiming at obtaining knowledge on the polyelectrolyte component in the LB film. Measurements of UV absorption spectra of APS of the transferred films confirmed an important aspect that a monomolecular film formation of the polyelectrolyte is fulfilled in the polyion complex LB film. More importantly, the optical evaluation provided new insights on the conformational and orientational state of the polyelectrolyte component.

Structural and morphological features of the polyion complex films can be extracted in comparison with those of the amphiphilic analogue (C_{18}APS). Major differences between these films are the transfer modes (Y- or Z-type) which are then correlated to the structural stability after deposition, the homogeneity of the film morphology, the quality of the bilayer stacks, and the surface smoothness. Also, the plausible location of the Si main chain in the LB films is supposed to be different. We assume that the dimension of the APS unit is uncorrespondingly large for occupying areas of ordinary amphiphiles, and this should lead to disordering of the film structures and unsuccessful deposition. Polysilane electrolytes having a more refined structure with a smaller unit would be required to make honest comparisons with studies using widely employed polyelectrolytes.

References and Notes

(1) Goddard, E. D.; Hannan, R. B. *J. Colloid Interface Sci.* **1976**, *55*, 73.
(2) Shimomura, M.; Kunitake, T. *Thin Solid Films* **1985**, *132*, 243.
(3) Higashi, N.; Kunitake, T. *Chem. Lett.* **1986**, 105.
(4) Kunitake, T.; Higashi, N.; Kunitake, M.; Fukushige, Y. *Macromolecules* **1989**, *22*, 485.
(5) Nishiyama, K.; Fujihira, M. *Chem. Lett.* **1988**, 1258.
(6) Nishiyama, K.; Kurihara, M.; Fujihira, M. *Thin Solid Films* **1989**, *179*, 477.
(7) Umemura, J.; Hishiro, Y; Kawai, T.; Takenaka, T.; Gotoh, Y.; Fujihira, M. *Thin Solid Films* **1989**, *178*, 281.
(8) Takahara, A.; Moritomi, N.; Hiraoka, S.; Higashi, N.; Kunitake, T.; Kajiyama, T. *Macromolecules* **1989**, *22*, 617.
(9) Kajiyama, T.; Zhang, L.; Uchida, M.; Oishi, Y.; Takahara, A. *Langmuir* **1993**, *9*, 760.
(10) Erdelen, C.; Laschewsky, A.; Ringsdorf, H.; Schneider, J.; Schuster, A. *Thin Solid Films* **1989**, *180*, 153.
(11) Kimizuka, N.; Kunitake, T. *Chem. Lett.* **1988**, 827.
(12) Chi, L. F.; Johnston, R. R.; Ringsdorf, H. *Langmuir* **1991**, *7*, 2323.
(13) Lee, B.-J; Kunitake, T. *Langmuir* **1994**, *10*, 557.
(14) Overney, R. M.; Meyer, E.; Fromer, J.; Güntherodt, H.-J.; Fujihira, M.; Takano, H.; Gotoh, Y. *Langmuir* **1994**, *10*, 1281.
(15) Miyano, K.; Asano, K.; Shimomura, M. *Langmuir* **1991**, *7*, 444.

(16) Lee, E. M.; Kanelleas, D.; Milnes, J. E.; Smith, K.; Warren, N.; Webberley, M.; Rennie, A. R. *Langmuir* **1996**, *12*, 1270.
(17) For reviews see: (a) Michl, J.; Miller, R. *Chem. Rev.* **1989**, *89*, 1359. (b) West, R. *J. Organomet. Chem.* **1988**, *24*, 5068.
(18) Seki, T.; Tamaki, T.; Ueno, K. *Macromolecules* **1992**, *25*, 3825.
(19) Seki, T.; Tamaki, T.; Ueno, K.; Tanaka, Y. *Thin Solid Films* **1994**, *243*, 625.
(20) Seki, T.; Tanigaki, N.; Yase, K.; Kaito, A.; Tamaki, T.; Ueno, K.; Tanaka, Y. *Macromolecules* **1995**, *28*, 5609.
(21) Embs, F. W.; Wegner, G.; Neher, D.; Albouy, P.; Miller, R. D.; Wilson, C. G.; Schrepp, W. *Macromolecules* **1991**, *24*, 5068.
(22) Kani, R.; Yoshida, H.; Nakano, Y.; Murai, S.; Mori, Y.; Kawata, Y.; Hayase, S. *Langmuir* **1993**, *9*, 3045.
(23) Kani, R.; Nakano, Y.; Yoshida, H.; Majima, Y.; Hayase, S.; Yuan, C.-H.; West, R. *Macromolecules* **1994**, *27*, 1911.
(24) Preliminary results have already been reported: Seki, T.; Tohnai, A.; Tamaki, T.; Ueno, K. *J. Chem. Soc., Chem. Commun.* **1993**, 1876.
(25) Seki, T.; Tohnai, A.; Tamaki, T.; Kaito, A. *Chem. Lett.* **1996**, 361.
(26) Seki, T.; Sakuragi, M.; Kawanishi, Y.; Suzuki, Y.; Tamaki, T.; Fukuda, R.; Ichimura, K. *Langmuir* **1993**, *9*, 211.
(27) Smart, J. L.; McCammon, J. A. *J. Am. Chem. Soc.* **1996**, *118*, 2283.
(28) Kobayashi, K.; Takaoka, K.; Ochiai, S. *Thin Solid Films* **1988**, *159*, 267.
(29) Seki, T.; Tohnai, A.; Tamaki, T.; Kaito, A. *Macromolecules* **1996**, *29*, 4813.
(30) Schweigk, S.; Vahlenkamp, T.; Xu, Y.; Wegner, G. *Macromolecules* **1992**, *25*, 2513.
(31) Our unpublished result for the 49-layered cadmium arachidate film on a quartz plate and a value from the literature: Skita, V.; Richardson, W.; Filipkowski, M.; Garito, A.; Blasie, J. K. *J. Phys.* **1986**, *47*, 1849.
(32) Umemura, J.; Cameron, D. G.; Mantsch, H. H. *Biochim. Biophys. Acta* **1980**, *602*, 32.
(33) Katayama, N.; Ozaki, Y.; Seki, T.; Tamaki, T.; Iriyama, K. *Langmuir* **1994**, *10*, 1898.

MA960548J